Journal of Cleaner Production 369 (2022) 133176

Contents lists available at ScienceDirect

Journal of Cleaner Production

journal homepage: www.elsevier.com/locate/jclepro

An improved hourly-resolved NOx emission inventory for power plants based on continuous emission monitoring system (CEMS) database: A case in Jiangsu, China

Xuan Gu [a,b], Baojie Li [a,c,*], Chu Sun [a], Hong Liao [a], Yongqi Zhao [a], Yang Yang [a]

[a] Collaborative Innovation Center of Atmospheric Environment and Equipment Technology, Jiangsu Key Laboratory of Atmospheric Environment Monitoring and Pollution Control, School of Environmental Science and Engineering, Nanjing University of Information Science & Technology, Nanjing, 210044, China
[b] Shanghai Key Lab for Urban Ecological Processes and Eco-Restoration, School of Ecological and Environmental Sciences, East China Normal University, Shanghai, 200241, China
[c] Nanjing Xinda Safety Emergency Management Research Institute, Nanjing, 210044, China

ARTICLE INFO

Handling Editor: Cecilia Maria Villas Bôas de Almeida

Keywords:
CEMS
NOx
Emission inventories
Power plants
Week effect

ABSTRACT

High-resolved emission inventories are essential to evaluate air quality and health effects. However, for one of the most polluting industries in China – power plants, emission uncertainties remain high due to the limitation of point measurements. In this study, we established an hourly NOx emission inventory based on the continuous emission monitoring system (CEMS) network of Jiangsu, China, with an integrated new method that coupled unit-level fuel consumption and emission factors. To evaluate the accuracy of our method, we compared the accuracies of our method to three other bottom-up inventories and determined that, our results (CEMS (Improved) for which the normalized mean bias (NMB) was 3.24%) exhibited higher accuracies compared to the other two methods: BASE EIs and CEMS(Traditional), for which the NMB was −38.53% and 294.1%, respectively. The total NOx emissions of power plants in Jiangsu, China, were 43701 tons in 2018, equivalent to 42.2% of that in 2017. 53% of total emissions were contributed by the southern Jiangsu area and super units (>1000 MW) exhibited the largest emissions shares (70%). The daily, monthly, and hourly average emissions demonstrated a "high in winter and summer" pattern. The ratio of the highest daily emissions in the June-July-August period (JJA) to the lowest in the September–November period (SON) was 1.20, which is relatively higher than that of fuel consumption (1.18) and power generation (1.15). The weekly and monthly emissions on hourly trends varied consistently, with peaks at 12:00,16:00,19:00, and 21:00 (except for high-discharge months). The hourly emissions on holidays and weekends were 6.4% and 1.6%, lower than those of workdays and weekends, with emission disparities being the largest in the period of 8:00–10:00. Our new hourly CEMS emission inventory can significantly reduce the uncertainties of emission estimation and better serve policy-making for mitigating power plant emissions in China.

1. Introduction

Power plants in China have consistently been the primary sources of air pollution and coal consumption. In 2018, the coal consumption of China was 40.46 tons, with power sectors contributing 52%, equivalent to 50.5% of the global use (NBSC, 2019). From 2010 to 2017, power plants contributed 5.0–23.5% of PM, 15.7–38.7% of SO_2, and 19.1–51.5% of NOx in all the anthropogenic sources (Tang et al., 2020). Considering that further climate mitigation efforts (e.g., China's 2060 carbon neutrality goal) are required to significantly reduce the air pollution exposure of the Chinese majority (Cheng et al., 2021), power plants will require deep emission reduction over the next 30 years (Li et al., 2020). NOx is the key of several species involved in the formation of VOCs and O_3 (Atkinson, 2000; Sillman and West, 2009; Wang et al., 2019). As the precursor of nitrates, NOx plays a crucial role in the increase of important inorganic composition of $PM_{2.5}$ such as sulfate, nitrate, and ammonium (SNA), especially in autumn and winter (Huang et al., 2021; Ren et al., 2021; Wang et al., 2013, 2020). Furthermore,

* Corresponding author. School of Environmental Science and Engineering, Nanjing University of Information Science and Technology, Nanjing, 210044, China.
E-mail addresses: Belle824@163.com (X. Gu), baojieli@nuist.edu.cn (B. Li), sunchulyx@163.com (C. Sun), hongliao@nuist.edu.cn (H. Liao), 202212120020@nuist.edu.cn (Y. Zhao), yang.yang@nuist.edu.cn (Y. Yang).

https://doi.org/10.1016/j.jclepro.2022.133176
Received 23 December 2021; Received in revised form 22 June 2022; Accepted 14 July 2022
Available online 30 July 2022

NOx can result in hypertrophic water bodies (Jiang et al., 2020). In recent years, the Chinese government has developed a series of measures and regulations for power plants. For example, the ultra-low emission technologies were widely required for 60% of further emission reduction by 2020 (Bo et al., 2018). Contributed by the transformation of energy structures, the mitigating effects for NOx were significant (He et al., 2019; Lei et al., 2017). Establishing hourly-resolved gridded emission inventories could better explore mitigating effects caused by controlling measures.

For a long time, it has been fundamental to establish high spatio-temporal emission inventories for air quality models and policy regulations (Chen et al., 2019; Liu et al., 2015, 2017). With the demand for evaluating acute health effects of air pollution, high-resolved inventories become more crucial (Shen et al., 2017). Bottom-up method shows greater performances at fine scales, which reduces decoupling effects from emission facility locations and spatial surrogates (Bo et al., 2016). Recently, new accurate spatial allocation methods have been developed using various classes of technologies. For example, Li et al. (2019) established a $0.05^\circ \times 0.05^\circ$ gridded emission inventory for China in 2016 based on point-of-interest (POI) data that represent real geographical entities, which largely reduced the spatial bias for energy consumption. A suitable spatial proxy method could largely reduce the uncertainties of the emission estimates. However, traditional bottom-up emission inventories using population density, road networks, and other spatial proxies are largely dependent on the assumption that emissions and parameters are linearly correlated (Li et al., 2017; Nassar et al., 2013; Shi et al., 2016), which inevitably introduce modeling bias (Chen et al., 2014; Zhao et al., 2008; Zheng et al., 2021). In addition, studies have shown that thermal power generation and cogeneration power plants have great potential to reduce coal consumption, in which the capacity utilization rate and annual utilization hours are crucial (Cui et al., 2021; Nakaishi et al., 2021). It is the direction of efforts to apply real-time emission parameters from the individual plant when establishing high-resolution emission inventories.

High resolution emission inventories using bottom-up method require rich and detailed records of energy use, facility locations, and other socioeconomic datasets from multiple regional and temporal scales (Cai et al., 2018). In recent years, power plants, pulverized coal-fired boilers, oil-fired boilers with an output of more than 65 tons of steam per hour, as well as gas turbines, are required to install the continuous emission monitoring system (CEMS), according to "Emission Standard of Air Pollutants for Thermal Power Plants (GB13223-2011)". The national CEMS network can avoid the uncertainty of average emission factors acquired from empirical parameters by offering detailed, hourly frequency stack concentrations. The total installed capacity of CEMS accounts for 96.01%, 97.15%, and 95.91% of the power plants in 2014, 2015, and 2017, respectively (Tang et al., 2020), which covers most of the power plants in China. As a consequence, the CEMS can function as a policy stringency to evaluate the overall mitigating effect on a fine scale. Tang et al. (2019) determined that emissions of NOx from power plants in China decreased by 60% between 2014 and 2017. Chen et al. (2019) found that ultra-low strategies reduced the emission factors of some pollutants by 1-2 orders of magnitude. Some parameters are unavailable or inadequate in CEMS measurements, such as flue gas volume. Under these circumstances, the existing CEMS-based inventories resorted to inventory-establishing methods that indirectly associated key parameters. One of these approaches estimated emissions by multiplying gas concentrations with fixed air volume, thereby failing to reflect the time-varying characteristics of power plant operations. Another method introduced theoretical smoke volume and activity levels based on fuel information to obtain emissions, which were derived from broad classes of activity levels. Furthermore, Karplus et al. (2018) observed that many plants in some key regions in China did not comply with the strictest new standard and suggested hourly reporting of emissions as part of national air pollution control efforts. Therefore, it is vital to establish hourly emission inventories with real-time emissions.

Our method is innovative in that we achieved a higher temporal resolution of activity levels based on multiple datasets. The power plants in Jiangsu were noticeable. In 2018, the power generation in Jiangsu was 4933.5×10^8 kWh, with the total installed capacity ranking first in China. It is crucial to estimate power plant emissions in Jiangsu. The main aims of this study were to: (1) improve the spatial allocation of unit-specific activity levels for power plants, and devise an hourly NOx emission inventory for Jiangsu in 2018; (2) take Wuxi, Jiangsu Province as an example, compare three inventory methods and quantify the improvement of accuracy in our method; and (3) explore the emission characteristics of NOx at monthly, weekly, diurnal, hourly, and spatial levels. Our inventories with high-resolved activity levels could largely improve the accuracy of power plant emission estimates. The results of hourly real-time emissions could enable decision-makers to formulate precautionary measures for short-time air pollution control in China, especially during important issues or events (e.g., Asian Games).

2. Methods and materials

2.1. Study area

Jiangsu Province (30°45′–35°20′N, 116°18′–121°57′E) is located in one of several large city clusters, the Yangtze River Delta (YRD) (Fig. 1). In 2018, its contribution to 10.3% of the gross domestic product in China emerged from important economic branches in the country. Recently, air contamination in Jiangsu remained serious). According to "2018 World Air Quality Report: Region and City $PM_{2.5}$ Ranking" (AirVisual, 2018), the top 15 of the most polluted regions in East Asia were all in China, mainly in BTH (Beijing-Tianjin-Hebei) and YRD, with an average annual $PM_{2.5}$ mean concentration of 74.9 μg/m^3. In 2018, coal consumption in Jiangsu reached 254.07 million tons, ranking fifth in China, while the shares of gas and oil consumption (15.85%) and non-fossil fuel consumption (7.83%) were lower than the nationwide averages. Herein, we divided Jiangsu Province into three regions: northern Jiangsu area (NJS, including Lianyungang City, Xuzhou City, Suqian City, Huaian City, Yancheng City), Central Jiangsu Area (CJS, including Yangzhou City, Taizhou City, Nantong City), and Southern Area (SJS, including Nanjing City, Zhenjiang City, Changzhou City, Wuxi City, Suzhou City).

2.2. The new method for CEMS-based inventories — CEMS(Improved)

2.2.1. The improvement of activity levels and emission factors

Activity levels. In general, fine-scale bottom-up emission inventories for power plants require other detailed parameters for activity

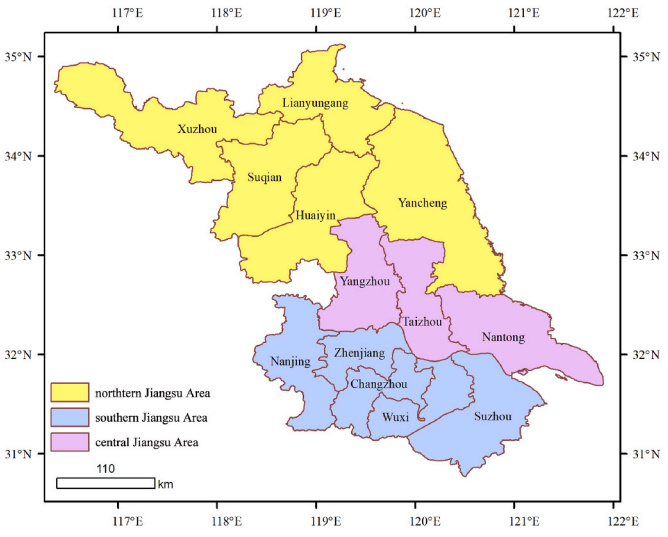

Fig. 1. Location of sampling sites in Jiangsu Province, China.

levels. Liu et al. (2015) introduced the definition of "power generation ability" which significantly reduced the uncertainties of fuel consumption estimated by unit sizes and fuel types. In this study, parameters of Eqs. (1)-(3) were improved for activity levels, owing to which the hourly-resolved data were displayed. The fuel types in this study were coal, gas and oil, biomass, and other fuels.

$$A_i = G_i \times opT_i \tag{1}$$

$$G_i = U_i \times P \times H_0 / H_j \tag{2}$$

$$opT_i = \sum T_i \Big/ n_i \times f \tag{3}$$

where i represents the power plant, j represents the fuel type, A is the fuel consumption, in 10^4t (gas is 10^4 m^3), G is the power generation ability, U is the unit installed capacity in MW, P is the fuel consumption rate presented in grams of coal equivalent per kWh supplied (gce kWh^{-1}), H_j is the heating value of fuel types used for each unit in kJ g^{-1}, and H_0 is the heating value of standard coal. T is the CEMS monitoring in hours, which is equivalent to operating hours for power plants, opT_i is the annual average utilization hours at each outlet in a power plant, n is the outlet in a power plant, f is the average load rate, equivalent to the conversion coefficient of power generation utilization hours and operating hours, which is taken as 1.70.

Emission factors. The calculation for emission factors are shown in Eqs. (4)-(6) (Zhao et al., 2010). For fuel types that lacked theoretical smoke volume, we usedthe measured values in 2015 (Tang et al., 2019).

$$EF_{i,k} = C_i \times V_k \tag{4}$$

$$C_{AVE,i} = \sum_j \sum_h C_{j,h} \Big/ \sum_j T_j \tag{5}$$

$$V = 1.04 \times Q_L/4186.8 + 0.77 + 1.0161 \times (\alpha - 1) \times V_0 \tag{6}$$

where EF represents the emission factor (in g/kg per fuel); i represents power plants; j represents the outlet in a power plant; k is the fuel type; C_{AVE} is the average concentration (mg/m^3); T is the CEMS monitoring in hours; Q_L is the lower heating value (kJ/kg); V is the theoretical smoke volume (m^3/kg); α is the excess air coefficient (1.4); V_0 is the theoretical air volume (5.525908 m^3/kg) (Zhao et al., 2010).

2.2.2. The CEMS datasets

This study collected the CEMS datasets of power plants in Jiangsu from (http://218.94.78.61:8080/newpub/web/home.htm), with a combined installed capacity of 95611.95 MW, accounting for 99.8% of the total. The NOx concentrations of the units were obtained on an hourly basis. To determine the operating time of each plant and its power generation hours, we conducted quality control on measured concentrations according to the CEMS technical requirements, including eliminating negative values, outlier values, and null values. The "Specifications for continuous emissions monitoring of SO2, NOX, and particulate matter in the flue gas emitted from stationary sources (HJ/T75-2017)" were used as a reference to complement the arithmetic mean values of valid data. In addition, there was a period of one month for most power plants when the emission concentrations were invalid or zero, which we regarded as the shutdown period of power plants.

For power plants without the installation of CEMS, we used monthly-averaged power generation hours and concentrations to calculate the monthly NOx emissions inventories. The data processing of this part had little impact on our whole emission inventory because the installed capacity of them only accounted for 0.02% of the whole units.

2.3. Other methods for bottom-up emission inventories — BASE EIs and CEMS(Traditional)

2.3.1. The traditional method: BASE EIs

As previously stated, traditional methods for bottom-up inventories generally assume that emissions are linearly correlated with energy consumption or other economic statistics. Furthermore, the emission factors were the results of invariable statistics, and the activity levels were at aggregated scales. For areas where we could hardly obtain unit-level data, we estimated the emissions according to the energy data in the municipal statistical yearbook (Fu et al., 2013; Xia et al., 2016). The emissions were calculated using Eq. (7)

$$E = \sum_{i,k} A_{i,k} \times EF_{j,k} \tag{7}$$

where i, j and k represent the region, unit, and fuel type, respectively; E is the total emissions; $A_{i,k}$ is the activity level (fuel consumption), which was linearly correlated with the unit size of each plant according to the provincial fuel consumption-related parameters (NBSC, 2019), $EF_{j,k}$ is the emission factor, in mg/m^3, which considers the removal efficiencies of different fuel types and technologies.

2.3.2. CEMS-based method involving fixed smoke emissions: CEMS (Traditional)

Unlike the theoretical fuel gas rates and emission factors obtained by heating values of different fuel types in *2.2.1*, previous studies offered another method that resorted to the outlet air volume under standard conditions, multiplied by the CEMS concentrations ((Chen et al., 2019)). The emissions were calculated with Eq. (8). The merit of this method is, to some extent, that it reduces distortion of the estimated fuel gas volume, while the limitation was apparent owing to its dependence on extra measurement parameters (Gilbert and Sovacool, 2017), which will be discussed in *Section 3.1.1*.

$$E_i = C_i \times Q_{sn} \times T_i / 1000000 \tag{8}$$

where E_i represents the total emissions (kg/h), i represents the emission outlets, C_i is the average concentration, and Q_{sn} is the fixed fuel gas volume under standard conditions (m^3/h).

2.4. Accuracy evaluation of the improved NOx emission inventory

To verify the accuracy of the optimization results in Section 2.2, we used the actual fuel consumption of power plants to estimate the actual emissions obtained by the environmental survey data in Wuxi in 2018. Two statistical parameters, bias (BIAS) and normalized mean bias (NMB), were introduced to evaluate the monthly modeling bias of BASE EIs, CEMS(Traditional), and CEMS(Improved). In addition, we also compared the monthly disparities of the results using the coefficient of determination (R^2). In addition, to compare the results from different studies, we also comprehensively investigated the concentrations, emission factors and emissions from relevant literature.

3. Results and discussions

3.1. Model validation and comparison of results

3.1.1. Accuracy verification of different methods - a case in Wuxi, Jiangsu Province

The monthly emissions and model performance of Wuxi's power plants in Jiangsu Province are analyzed. The actual emissions from 26 power plants in Wuxi were 3780.6 t, and the modeling results by our studies were: CEMS(Improved) 3901.8 t, CEMS(Traditional) 2307.3 t, and BASE EIs 17332.4 t (Table 1). The largest discrepancies between actual and modeling emissions occurred in February and December by CEMS(Improved) and BASE EIs, and in July and September by CEMS

Table 1
Monthly emissions of different methods in Wuxi, Jiangsu.

Months	CEMS (Improved)	Actual Emissions	CEMS (Traditional)	BASE EIs
Jan.	381.48	362.04	232.32	1434.4
Feb.	221.29	260.79	172.36	1433.0
Mar.	285.90	312.26	201.73	1440.5
Apr.	355.36	337.03	202.35	1361.4
May.	299.95	317.97	195.40	1344.5
Jun.	278.81	279.29	170.15	1392.9
Jul.	349.76	335.60	192.46	1525.9
Aug.	354.22	336.47	195.82	1760.1
Sep.	360.17	329.91	184.56	1425.8
Oct.	328.30	313.89	197.65	1310.8
Nov.	345.92	302.78	194.16	1317.6
Dec.	340.65	292.60	168.35	1585.3
Total	3901.8	3780.6	2307.3	17332.4

Table 2
Statistical parameters for three different methods.

Month	BASE EIs		CEMS(Traditional)		CEMS(Improved)	
	BIAS	NMB	BIAS	NMB	BIAS	NMB
Jan.	32.34	232.28%	−4.99	−35.83%	0.75	5.37%
Feb.	39.97	398.46%	−3.40	−33.91%	−1.52	−15.15%
Mar.	34.46	286.90%	−4.25	−31.10%	−1.01	−8.44%
Apr.	30.95	238.75%	−5.18	−39.96%	0.70	5.44%
May.	31.14	254.62%	−4.71	−38.55%	−0.69	−5.67%
Jun.	34.19	318.26%	−4.20	−39.08%	0.40	3.44%
Jul.	42.48	329.10%	−5.51	−42.65%	0.54	4.22%
Aug.	43.83	338.70%	−5.41	−41.80%	0.68	5.28%
Sep.	33.30	262.46%	−5.59	−44.06%	1.16	9.17%
Oct.	30.21	250.24%	−4.47	−37.03%	0.55	4.59%
Nov.	30.86	264.97%	−4.18	−35.87%	1.66	14.25%
Dec.	39.88	354.39%	−4.78	−42.46%	1.85	16.42%

(Traditional). BASE EIs without considering the latest dust removal devices displayed 3.9 times the emissions from actual energy data. CEMS (Traditional) underestimated the emissions primarily owing to the fixed flue gas volume, which ignored the outlet parameters affected by complicated conditions. The monthly emissions of the CEMS(Improved) and CEMS(Traditional) were compared with actual emissions in Fig. 2. The slopes of CEMS(Improved), CEMS(Traditional) and BASE EIs were 1.30, 0.51, and 0.76, with R^2 values of 0.70, 0.67, and 0.03, respectively. This indicates that the fuel consumption at unit levels exerted a significant effect on improving the accuracy of the emission inventory in high-energy-consuming plants.

Table 2 uses two statistical parameters to test the accuracy of the three methods. The average BIAS of the CEMS(Improved) of 12 months was 0.4%, which was 10 and 100 times lower than that of the CEMS (Traditional) (−4.7%) and BASE EIs (35.3%). The largest discrepancies between actual and modeling emissions occurred in February and December by CEMS(Improved) and BASE EIs, and July and September by CEMS(Traditional). Compared with the other methods, CEMS (Improved) showed a higher accuracy in summer.

3.2. The spatial distribution of NOx emissions for power plants

The spatial distribution of the annual NOx emissions of the power plants and their installed capacities is shown in Fig. 3. Regional disparities in emissions are also displayed (Fig. 4). The proportions of total emissions in the northern Jiangsu area (NJS), southern Jiangsu area (SJS), and central Jiangsu area (CJS) were basically consistent with their total installed capacity, which were 1229.8 t, 23262.0 t, and 8209.3 t, respectively. The highest emissions in the three areas occurred in Xuzhou (5627 t), Suzhou (8125 t), and Taizhou (4051 t). The ratio of the highest emissions throughout Jiangsu in Suzhou to the lowest in Huaian was 11.6. The total emissions of units: small (<300 MW), middle (300–600 MW), large (600–1000 MW), and super (>1000 MW) were 7253 t, 942 t, 3320 t, 32186 t, respectively. Units ≥ 600 MW dominated the emissions as the primary source of the contribution, which was mainly distributed in Xuzhou and SJS, contributing to 81.2% of Jiangsu's emissions. The super units (>1000 MW) may explain the situation in which emissions in SJS (23262 t) were twice that in NJS (12230 t): In NJS, there was an emission of 9228.8 t by 13 super units with a combined installed capacity of 22030 MW, while in SJS there was 16128.6 t by 19 super units with a combined installed capacity of 32507 MW. Generally, the emission disparities at regional scales are the result of population density, economic development, and industry structures (Zhou and Zhao, 2015). Tong et al. (2018) also found that coal-fired units with large installed capacity always had large fractions of emissions.

As shown in Fig. 5, for super units, the shares of emissions, fuel consumption, and installed capacities were all considerable, which stood at 73.6%, 69.9%, and 76.0%, respectively. In contrast, for small units, the share of power generation in Jiangsu was 9.4%, close to that of units <100 MW in 2010 at the national level. Tong et al. (2018) observed that in units<100 MW, the emission share was higher than the electricity generation share. In our study, the proportion was 16.6% of emission, 6.8% of installed capacity, and 13.9% of fuel consumption. In terms of the emission concentrations, the values of four unit groups were: 46.9 mg/m^3 of small units, 25.9 mg/m^3 of middle units, 27.5 mg/m^3 of large units, and 31.6 mg/m^3 of super units. The small units took the lead, which could be explained by their large quantity throughout the province with an uneven distribution of controlling technologies. Furthermore, the distribution of emission factors from all power plants in Jiangsu compared with the installed capacity for each unit is presented in Fig. 5 (b). Units of < 600 MW accounted for 80% in number, with an average emission factor of 0.40 g/kg, which was slightly higher than the average values of all the units (0.38 g/kg). It is evident that the emission factors decreased with an increase in the unit capacity. This was consistent with Dai (2016) and Zhang et al. (2018), and was reasonable because of the impacts of the revolution of operating and controlling technologies on small units. The disproportionalities of emissions and overall installed capacities among different unit groups could be attributed to the mixed factors of rigorous emission strategies for all levels of units and the relatively high cost of advanced controlling technologies installation on the existing smaller units (Tong et al., 2018).

The annual emission ranges by the unit of different fuel types are shown in Fig. 6. It is apparent that the energy structure of Jiangsu was

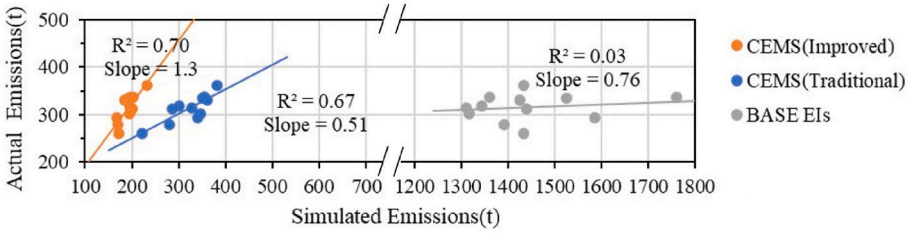

Fig. 2. The correlations between modeling results and actual emissions in Wuxi, Jiangsu.

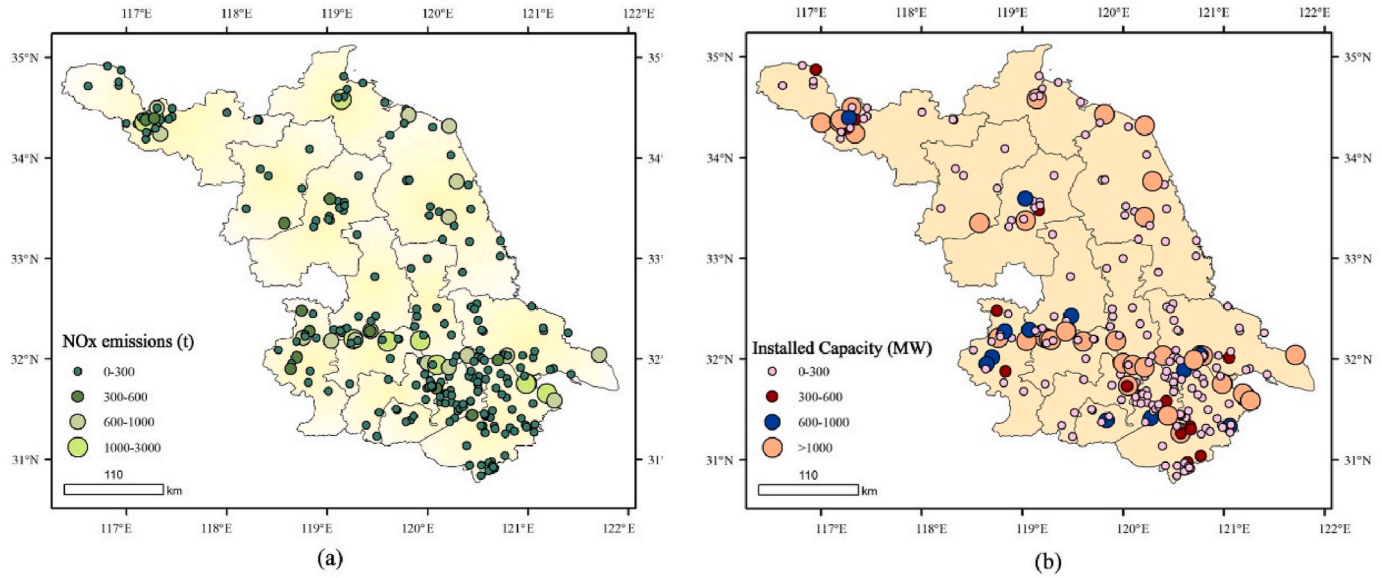

Fig. 3. Spatial distribution of (a) NOx emissions, (b) Installed capacities in Jiangsu.

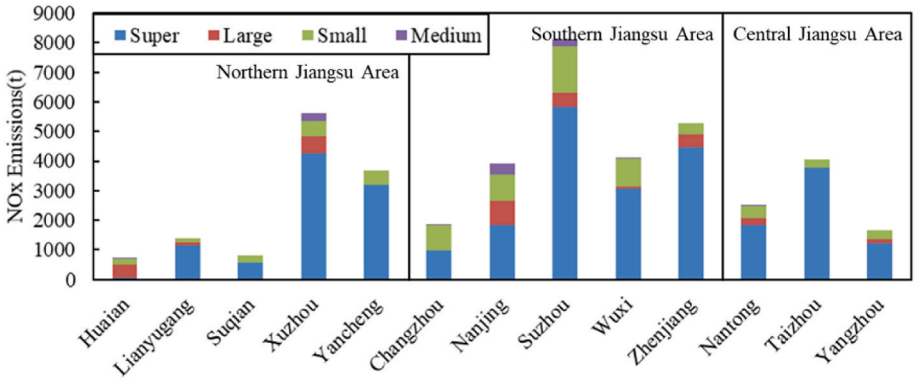

Fig. 4. Regional distribution of emissions of varied unit capacity sizes (super, large, small, and medium represent units of <300, 300–600, 600–1000, and > 1000 MW, respectively).

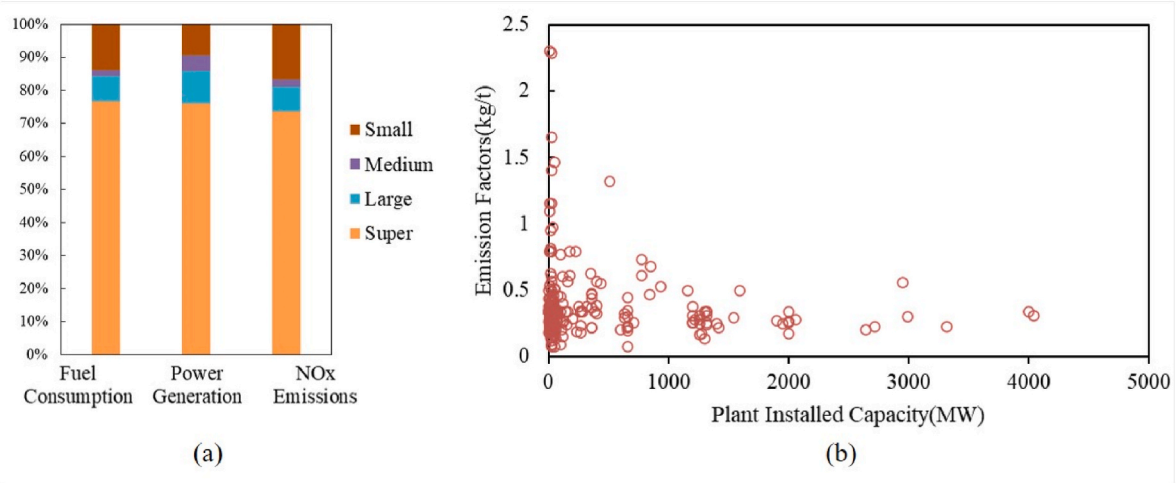

Fig. 5. (a) Shares of emissions, fuel consumption, and power generation by unit groups. (b) Distribution of emission factors by unit capacity.

still dominated by coal, with emissions of 71%, 94%, 96%, and 99% in small, middle, large, and super units, respectively. The average emissions of units from small-to super-size were 36.1 t (0.11–561 t), 76.8 t (2.08–353 t), 195.3 t (8.56–467 t), and 847.0 t (22.5–2831 t), respectively. The structure of emissions from 4 kinds of unit sizes was different from that of other well-developed regions. For example, in our results,

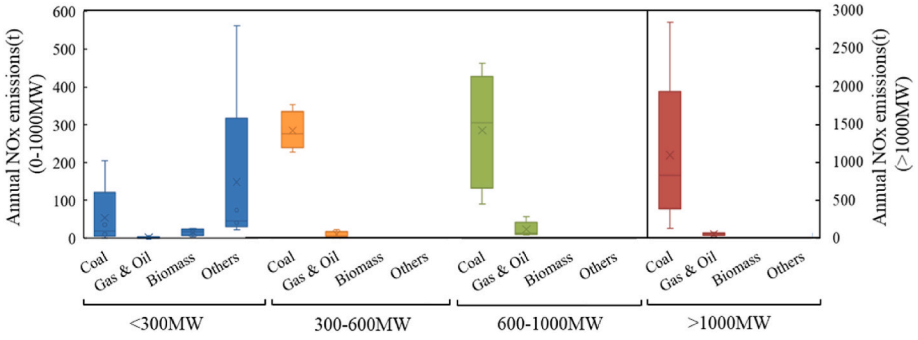

Fig. 6. Emission ranges in different fuel types of unit groups.

units >1000 MW displayed a much broader emission range than that in Shanghai in Chen et al. (2019), which were all lower than 500 t. However, the emission range if units<300 MW exceeded that of medium (300–600 MW) and large (600–1000 MW) units, which was different from the results in Chen et al. (2019). From the perspective of fuel types, the average emissions of coal-, gas & oil-, biomass-, and other-fuel-burning plants were 196.4 t, 12.6 t, 15.7 t, and 116.2 t, respectively. The emission range of biomass burning plants was similar to that of gas and oil-burning plants, and contributed 26% of emissions for small units, which indicates their homologous technology promotion. Other-fuel-burning plants were all concentrated on units < 300 MW, while the emission distribution had a higher degree of dispersion (Q = 16.96 t). This indicates that the dispersion of power plants that did not generate electricity in traditional ways was small. Furthermore, plants that contributed disproportionately to the emissions and lacked cost-effective pollution control strategies could be shut down or transformed as part of efforts to reduce regional air pollution.

3.3. Characteristics of NOx emissions of power plants on varied temporal scales

3.3.1. Characteristics of NOx emissions on diurnal and monthly scales

The highest NOx emission for power plants in 2018 was 4316.6 t in August, and the lowest was 3039.9 t in November, with a ratio of 1.4, consistent with Chen et al. (2019). This ratio in MEIC (the Multi-resolution Emission Inventory for China, http://www.meicmodel.org) was 1.35, and the highest was January and the lowest was February in 2017. The emission shares in summer and winter accounted for 26.4% and 25.4%, respectively, of the entire year. We divided the provincial average emissions and activity levels into quarters and obtained the coefficient of variation (CV) (Table 3). The ranking of daily emissions and activity levels was JJA > DJF > MAM > SON. The ranking of CV was JJA > DJF > SON > MAM. The ratio of the highest emissions, fuel consumption, and power generation in JJA to the lowest in SON was 1.20, 1.18, and 1.15, respectively. The ranking of CVs in DJF and SON was emissions > fuel consumption > power generation, while in JJA was fuel consumption > emissions > power generation, and in MAM it was, power generation > emissions > fuel consumption.

Table 3
The seasonal emissions, fuel consumption, power generation, and CV.

Seasons		NOx Emissions /t	Fuel Consumption /10^4t	Power Generation /10^4kWh
DJF	Mean ± STD	3708.6 ± 444.6	1256.8 ± 99.4	499.6 ±45.0
	CV/%	11.99	7.91	9.01
MAM	Mean ± STD	3563.6 ±78.6	1187.2 ± 17.2	471.1 ± 15.8
	CV/%	2.21	1.45	3.36
JJA	Mean ± STD	3964 ±538.1	1385.4 ± 204.9	541.6 ± 67.6
	CV/%	13.58	14.79	12.49
SON	Mean ± STD	3297.7 ± 294.9	1168.1 ± 81.3	468.9 ± 33.0
	CV/%	8.94	6.96	7.04

Note: DJF, MAM, JJA, SON represent December-January-February, March-April-May, June-July-August, September-October-November.

On the daily scale, the CVs of emissions, fuel consumption, and power generation were 7.9%, 8.8%, and 8.0%, respectively, which were lower than those on the monthly scale, which were 11.3%, 10.9%, and 9.9%, respectively (Fig. 7). During the winter (January, February, and December in 2018) and spring in Jiangsu Province, the days with relatively high emissions did not necessarily correspond to the days with relatively high fuel consumption and electricity load. In summer, the emission peaks reached the highest, which was similar to the highest activity levels case. The emissions decreased significantly during the Spring Festival (from Feb 15th to Feb 21st) but fluctuated around high values from late July to mid-August. Taking Nanjing, Jiangsu Province as an example, the highest temperatures from Jul 24th to Jul 31st ranged from 35 °C to 37 °C. In August, the period of the highest temperature was from Aug 5th to Aug 11th, ranging from 35 °C to 36 °C. In winter, there was also a period in which the lowest temperatures ranged from −7 °C to −3 °C thereby reaching the monthly lowest values. As shown in Table 4, high emission values occurred at these extreme temperatures.

The average hourly NOx emissions in Jiangsu, China for each month in 2018 are displayed in Fig. 8. The average emissions were highest in August, July, and January, and lowest in November and April. The ratio of the highest emissions in August to the lowest in November was 1.2. The fluctuation of the emission trend was the largest in July (STD: 1.047 kg), followed by December (STD: 0.847 kg) and August (STD: 0.943 kg). The fluctuations of the emission trends in March, April, and May were relatively low (STD: 0.382–0.424 kg). This suggests the high sensitivity in handling the increased electrical load during the relatively cold and hot periods. The average emissions in April, May, June, July, and August peaked at 12:00, with the highest values occurring in summer. This indicates the influence of high temperatures and demand on electricity use. Other emission peaks of monthly patterns were 16:00, 19:00, and 21:00 (except for February, May, June, July, and December, which may be related to the seasonal emission trends). The emission valleys were at 8:00 and 11:00. This was largely because the power plant system has certain temporal fluctuations in access to the best power generating benefits.

3.3.2. The "week effect" and "holiday effect"

There were some hourly emission disparities that we regarded as "week effect" and "holiday effect" between weekdays and weekends as well as official holidays and workdays, which few studies have considered on a fine scale (Fig. 9). Official holidays refer to the rest days approved by the State Council, including New Year's Day, Spring Festival, Tomb-sweeping Day, Labor Day, Dragon Boat Festival, Mid-Autumn Festival, and National Day. The emission peaks in "week effect" patterns occurred at 12:00,16:00 and 21:00, similar to the seasonal

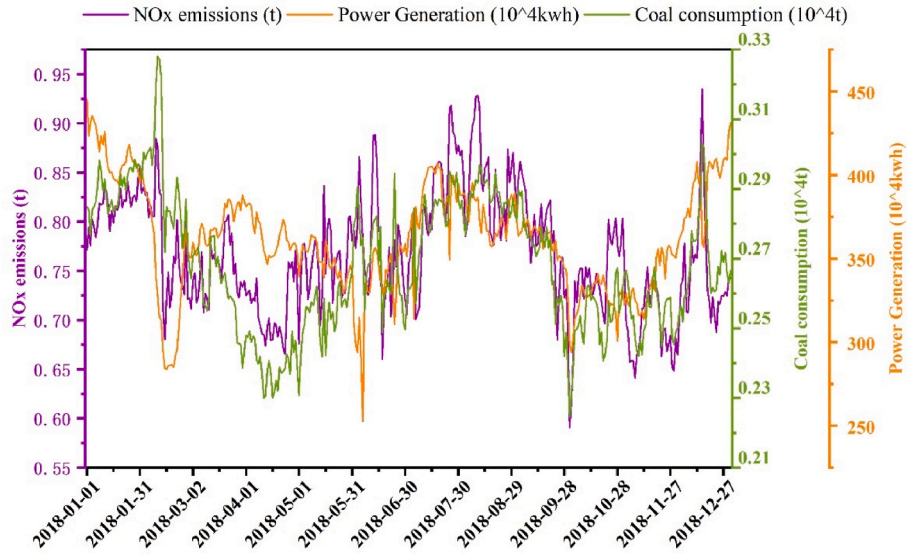

Fig. 7. Average daily NOx emissions, fuel consumption, and power generation in Jiangsu.

Table 4
Typical periods of provincial average emissions and activity levels.

Date	Power generating hours/h	Fuel consumption/10^4t	NOx emissions/t	Power generation/10^4 kWh	Features
2018-01-24	11.77	0.29	0.84	415.22	The low-temperature period in Nanjing
2018-01-25	11.85	0.30	0.83	418.24	
2018-01-31	11.20	0.30	0.86	395.01	
2018-02-02	11.18	0.30	0.84	394.73	
2018-02-15	8.04	0.28	0.72	283.81	The Spring Festival
2018-02-16	8.10	0.28	0.75	285.83	
2018-02-17	8.11	0.28	0.71	286.10	
2018-02-18	8.12	0.28	0.73	286.51	
2018-02-19	8.08	0.28	0.76	285.03	
2018-02-20	8.27	0.29	0.76	291.63	
2018-02-21	8.39	0.29	0.80	295.94	
2018-08-07	11.21	0.29	0.90	395.57	The high-temperature period in Nanjing
2018-08-09	10.90	0.29	0.93	384.45	
2018-08-10	10.95	0.29	0.93	386.49	
2018-08-11	10.58	0.30	0.92	373.23	
2018-10-01	8.47	0.22	0.59	298.83	The National Day holidays
2018-10-02	8.34	0.23	0.62	294.08	
2018-10-03	8.58	0.24	0.66	302.69	
2018-10-04	8.89	0.25	0.74	313.73	
2018-10-05	8.99	0.25	0.72	317.04	
2018-10-06	9.07	0.25	0.75	320.14	
2018-10-07	9.31	0.25	0.75	328.42	

patterns. The mean value of hourly emissions on holidays was (30.10 ± 0.77) kg, 6.4% lower than (32.13± 0.52) kg on workdays. On weekends and weekdays, the mean values were (31.62± 0.49) kg and (32.13± 0.57) kg, with differences of 1.6%. The largest emission gap between holidays and workdays was noted at 8:00, 9:00, and 11:00, similar to that on weekends and weekdays, which was partly caused by the discrepancies in lifestyles of citizens between work and spare time.

Chen et al. (2019) also determined that hourly NOx emissions on weekdays were higher than those on weekends (6–9%). In contrast to Fig. 9 (a), Chen et al. (2019) observed that the average emission on weekdays was only higher than on weekends during 6:00–17:00, with the smallest discrepancies at the beginning and the end. The slight differences in Fig. 9 (a) before 5:00 probably suggest the effectiveness of shut-down policies for power plants, while the emission pattern shifting on "week effect" at 6:00 and 17:00 in Chen et al. (2019) can be explained by the water transport routine in Shanghai.

3.4. Emissions compared with other studies

The annual emissions in this study compared with other studies are listed in Table 5. The total NOx emissions from CEMS(Improved) in 2018 were 43701 t, which is significantly lower than that of traditional methods (185.8 Gg). The proportion of installed capacity of power plants (99.8%) in our study is the highest among all the CEMS studies and MEIC. There were some discrepancies among the three CEMS inventories. The average emission factor of CEMS(Improved) was 94% lower than that of BASE EIs, which suggests the merit of the CEMS database in reducing the uncertainty of parameters such as installation rates and removal efficiencies of control technologies. The emission factors in the traditional method – BASE EIs, were determined based on field measurements (Tang et al., 2019). In our study, the CEMS system was comprehensively facilitated nationwide owing to ultra-low emission techniques (GOSC, 2016; Li et al., 2020). The annual NOx emissions in these studies, were approximately twice those of our study mainly owing to the average concentration in our study in 2018 being 59.6% of that in 2015, which was also lower than the sampling results (70–162 mg/m^3)

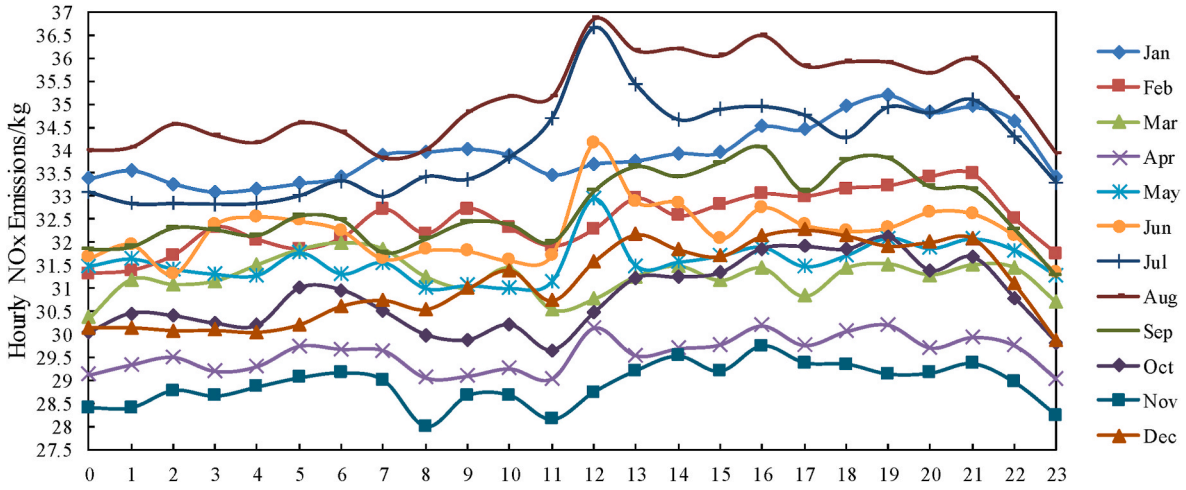

Fig. 8. Variation of average NOx emissions over 24 h for each month.

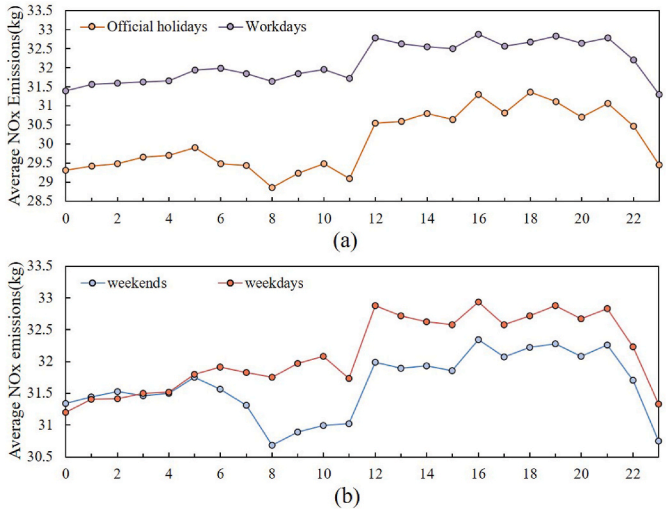

Fig. 9. Hourly variations for NOx emissions: (a) "week effect", (b) "holiday effect".

(Zhang et al., 2019). Also, the emission factors were lower than those in Guangdong Province (0.77–4.57 g/kg in 2011) (Dai, 2016) and China (0.48 g/kg in 2015), but nearly reached the average value in Shanghai (0.36 g/kg with a range of 0.09–1.87 g/kg) (Chen et al., 2019). Therefore, our results are more representative of the unit-level power plant emissions under ultra-low standards than other CEMS inventories, for example, Tang et al. (2019) and Zhang et al. (2019), both of which introduced the theoretical smoke volume with different preprocessing methods for CEMS concentrations.

4. Conclusion

Bottom-up emission inventories in China remain consistent with the challenges of relatively high emission uncertainties. Consequently, we developed a new method to establish an hourly NOx emission inventory and coupled energy consumption and emission factors. The modeling performances of our inventories are validated through real measurements of activity levels in Wuxi, Jiangsu. The CEMS(Improved) showed a higher modeling performance (R^2: 0.7, slope: 1.3) than CEMS(Traditional) (R^2: 0.67, slope: 0.51) and BAES EIs (R^2: 0.03, slope: 0.76). The average NMB of the CEMS(Improved) was 3.24%, superior to the CEMS (Traditional) (−38.53%) and BASE EIs (294.09%).

We investigated the effects of different fuel types and unit sizes on emissions. Small units (<300 MW) displayed larger emission shares than the activity levels because of higher emission concentrations and emission factors. Super units (>1000 MW) contributed to over 70% of emissions, fuel consumption, and power generation, which were the main forces of Jiangsu's power plants industry. These results can identify power plants that disproportionately contributed to emissions and fuel consumption, thereby helping reduce excess capacity in the power sector. We also revealed the characteristics of NOx emissions at varied temporal scales and offered the explanations. In 2018, the highest emission from power plants was in August (4316.6 t), and the lowest was in November (3039.9 t). The emission characteristics that peaked in summer and winter were more evident on diurnal and hourly scales. The provincial averages of activity levels and resultant emissions at the diurnal level were all higher in summer and winter (summer > winter) than in spring and autumn (autumn > spring). Cold and hot weather exerted an enormous influence on emissions and fuel consumption,

Table 5
Emission inventories for power plants from previous studies.

Period	Resolution	Method	Installed capacity /%	NOx concentrations/(mg/m^3)	Emission factors/(g/kg)	Emissions in Jiangsu/1000t
2018[a]	hourly	CEMS(Improved)	99.8% of CEMS	42.60	0.33	43.7
		CEMS(Traditional)		42.60	0.33	28.5
		Bottom-up			5.84	185.8
2017[b]	monthly	BASE EIs	>90% in China			318.6
2015[c]	monthly	CEMS(Traditional)	73%		0.92	107.5
		Bottom-up			2.85	344.6
2015[d]	daily	CEMS(Traditional)	98% in China	71.53	0.59	108.5
2012[e]	monthly	Bottom-up				277.9
2012[f]	monthly	BASE EIs				679.8

Note: a: this study, b: MEIC, c: Zhang et al. (2019), d: Tang et al. (2019), e: Yang et al. (2019), f: Zhou and Zhao (2015).

respectively, which exhibited the largest CVs. The provincial average emissions in the "week effect" and "holiday effect" peaked at 12:00, 16:00, and 21:00, which were slightly different in monthly patterns, indicating the seasonal disparities in hourly electricity demands. The average emissions on weekday patterns were higher than those on weekends. The results of our study were compared with other emission inventories. First, our study covering the highest shares of power plants with the hourly activity levels, enables governments to qualify reduction potentials brought by ultra-low technologies and mitigating measures. Second, our inventories can be applied to explore enterprise behaviors during holidays or events and whether they comply with new standards or regulations. Third, our inventories are useful to related studies focused on improving the spatial representatives of emission inventories based on socioeconomic datasets.

Our study was also subjected to several limitations. Firstly, due to the incomplete installation of CEMS, power plants that lacked CEMS data were not included in the hourly emission calculation, which accounted for only 0.02% of the total install capacity. Secondly, the emission factors for non-coal burning plants recommended from other studies may result in uncertainties in high spatiotemporal emissions but fortunately had a low emission range, which was 0.12–70.5 t, 4.24–15.4 t, and 22.1–561 t for gas & oil-, biomass-, and other-fuel-burning plants, respectively. We believe the hourly emission inventories can be applied in atmospheric chemistry models, and offer implications for air pollution prevention in China.

CRediT authorship contribution statement

Xuan Gu: Conceptualization, Investigation, Methodology, Writing – original draft, Writing – review & editing. **Baojie Li:** Conceptualization, Supervision, Resources, Writing – original draft, Writing – review & editing. **Chu Sun:** Methodology, Data curation. **Hong Liao:** Conceptualization, Supervision, Writing – review & editing. **Yongqi Zhao:** Investigation. **Yang Yang:** Investigation, Funding acquisition.

Declaration of competing interest

The authors declare that they have no known competing financial interests or personal relationships that could have appeared to influence the work reported in this paper.

Data availability

Data will be made available on request.

Acknowledgments

This study was supported by the National Key Research and Development Program of China [2020YFA0607803], the National Natural Science Foundation of China [42007381], and the Natural Science Foundation of Jiangsu Province [BK20200812 and BK20200515].

References

AirVisual, I., 2018. 2018 World Air Quality Report:Region and City PM2.5 Ranking. http://www.indiaenvironmentportal.org.in/files/file/world-air-quality-report-2018.pdf.

Atkinson, R., 2000. Atmospheric chemistry of VOCs and NO x. Atmos. Environ. 34 (12–14), 2063–2101.

Bo, Z., Qiang, Z., Dan, T., Chen, C., He, K., 2016. Resolution dependence of uncertainties in gridded emission inventories: a case study in Hebei, China. Atmos. Chem. Phys. 17 (2), 1–26.

Bo, Z., Dan, T., Meng, L., Fei, L., Qiang, Z., 2018. Trends in China's anthropogenic emissions since 2010 as the consequence of clean air actions. Atmos. Chem. Phys. 18 (19), 14095–14111.

Cai, B., Liang, S., Zhou, J., Wang, J., Cao, L., Qu, S., Xu, M., Yang, Z., 2018. China high resolution emission database (CHRED) with point emission sources, gridded emission data, and supplementary socioeconomic data. Resour. Conserv. Recycl. 129, 232–239.

Chen, X., Liu, Q., Sheng, T., Li, F., Xu, Z., Han, D., Zhang, X., Huang, X., Fu, Q., Cheng, J., 2019. A high temporal-spatial emission inventory and updated emission factors for coal-fired power plants in Shanghai, China. Sci. Total Environ. 688, 94–102.

Chen, L.H., Sun X.C., Y.Y., Zhang, Y.X., Zheng, C.H., Gao, 2014. Unit-based emission inventory and uncertainty assessment of coal-fired power plants. Atmos. Environ. 99, 527–535.

Cheng, J., Tong, D., Zhang, Q., Liu, Y., Lei, Y., Yan, G., Yan, L., Yu, S., Cui, R.Y., Leon, C., 2021. Pathways of China's PM2.5 air quality 2015–2060 in the context of carbon neutrality. Natl. Sci. Rev. 8 (12).

Cui, R.Y., Hultman, N., Cui, D., Mcjeon, H., Zhu, M., 2021. A plant-by-plant strategy for high-ambition coal power phaseout in China. Nat. Commun. 12 (1), 1–10.

Dai, P.H., 2016. The thermal power plants SO2 and NOx emission factor set and uncertainty analysis that based on the CEMS data. In: Master Thesis. South China University of Technology, Guangzhou, China (in Chinese).

Fu, X., Wang, S., Zhao, B., Xing, J., Cheng, Z., Liu, H., Hao, J., 2013. Emission inventory of primary pollutants and chemical speciation in 2010 for the Yangtze River Delta region, China. Atmos. Environ. 70, 39–50.

Gilbert, A.Q., Sovacool, B.K., 2017. Benchmarking natural gas and coal-fired electricity generation in the United States. Energy 134, 622–628.

GOSC (General Office of the State Council of PRC), 2016. Notice on the Implementation of Pollution Permit Management for the Thermal Power and Paper Industries and the Pilot Cities in the Beijing-Tianjin-Hebei Region.

He, S., Zhao, L., Ding, S., Liang, S., Liu, L., 2019. Mapping economic drivers of China's NOx emissions due to energy consumption. J. Clean. Prod. 241, 118130.

Huang, X., Tang, G., Zhang, J., Liu, B., Wang, Y., 2021. Characteristics of PM2.5 pollution in Beijing after the improvement of air quality. J. Environ. Sci. 100, 1–10.

Jiang, L., Chen, Y., Zhou, H., He, S., 2020. NOx emissions in China: temporal variations, spatial patterns and reduction potentials. Atmos. Pollut. Res. 11 (9), 1473–1480.

Karplus, V.J., Shuang, Z., Douglas, A., 2018. Quantifying coal power plant responses to tighter SO emissions standards in China. Proc. Natl. Acad. Ences. 115 (27), 7004–7009.

Lei, D., Chao, L., Chen, K., Huang, Y., Diao, B., 2017. Atmospheric pollution reduction effect and regional predicament: an empirical analysis based on the Chinese provincial NOx emissions. J. Environ. Manag. 196 (JUL.1), 178–187.

Li, M., Zhang, Q., Kurokawa, J.I., Woo, J.H., He, K., Lu, Z., Ohara, T., Song, Y., Streets, D. G., Carmichael, G.R., 2017. MIX: a mosaic Asian anthropogenic emission inventory under the international collaboration framework of the MICS-Asia and HTAP. Atmos. Chem. Phys. 17 (2), 935–963.

Li, B., Wang, J., Wu, S., Jia, Z., Li, Y., Wang, T., Zhou, S., 2019. New method for improving spatial allocation accuracy of industrial energy consumption and implications for polycyclic aromatic hydrocarbon emissions in China. Environ. Sci. Technol. 53 (8), 4326–4334.

Li, J., Cai, W., Li, H., Zheng, X., Wang, C., 2020. Incorporating health cobenefits in decision-making for the decommissioning of coal-fired power plants in China. Environ. Sci. Technol. 54 (21), 13935–13943.

Liu, F., Zhang, Q., Tong, D., Zheng, B., Li, M., Huo, H., He, K.B., 2015. High-resolution inventory of technologies, activities, and emissions of coal-fired power plants in China from 1990 to 2010. Atmos. Chem. Phys. 15 (23), 13299–13317.

Liu, S., Hua, S., Wang, K., Qiu, P., Tian, H., 2017. Spatial-temporal variation characteristics of air pollution in Henan of China: localized emission inventory, WRF/Chem simulations and potential source contribution analysis. Sci. Total Environ. 624, 396–406.

Nakaishi, T., Kagawa, S., Takayabu, H., Chen, L., 2021. Determinants of technical inefficiency in China's coal-fired power plants and policy recommendations for CO 2 mitigation. Environ. Sci. Pollut. Control Ser. 28 (37), 52064–52081.

Nassar, R., Napier-Linton, L., Gurney, K.R., Andres, R.J., Oda, T., Vogel, F.R., Deng, F., 2013. Improving the temporal and spatial distribution of CO2 emissions from global fossil fuel emission data sets. J. Geophys. Res. Atmos. 118 (2), 917–933.

NBSC (National Bureau of Statistics of China), 2019. China Energy Statistical Yearbook 2018. China Statistics Press, Beijing, China.

Ren, C., Huang, X., Wang, Z., Sun, P., Chi, X., Ma, Y., Zhou, D., Huang, J., Xie, Y., Gao, J., 2021. Nonlinear response of nitrate to NOx reduction in China during the COVID-19 pandemic. Atmos. Environ. 264, 118715.

Shen, Y., Wu, Y., Chen, G., Grinsven, H.V., Wang, X., Gu, B., Lou, X., 2017. Non-linear increase of respiratory diseases and their costs under severe air pollution. Environ. Pollut. 224, 631–637.

Shi, K., Chen, Y., Yu, B., Xu, T., Chen, Z., Liu, R., Li, L., Wu, J., 2016. Modeling spatiotemporal CO2 (carbon dioxide) emission dynamics in China from DMSP-OLS nighttime stable light data using panel data analysis. Appl. Energy 168, 523–533.

Sillman, S., West, J.J., 2009. Reactive nitrogen in Mexico City and its relation to ozone-precursor sensitivity: results from photochemical models. Atmos. Chem. Phys. 9 (11), 3477–3489.

Tang, L., Qu, J., Mi, Z., Bo, X., Zhao, X., 2019. Substantial emission reductions from Chinese power plants after the introduction of ultra-low emissions standards. Nat. Energy 4 (11), 929–938.

Tang, L., Xue, X., Qu, J., Mi, Z., Bo, X., Chang, X., Wang, S., Li, S., Cui, W., Dong, G., 2020. Air pollution emissions from Chinese power plants based on the continuous emission monitoring systems network. Sci. Data 7 (1), 1–10.

Wang, Y., Zhang, Q.Q., He, K., Zhang, Q., Chai, L., 2013. Sulfate-nitrate-ammonium aerosols over China: response to 2000–2015 emission changes of sulfur dioxide, nitrogen oxides, and ammonia. Atmos. Chem. Phys. 13 (5), 2635–2652.

Wang, N., Lyu, X., Deng, X., Huang, X., Jiang, F., Ding, A., 2019. Aggravating O 3 pollution due to NO x emission control in eastern China. Sci. Total Environ. 677, 732–744.

Tong, D., Zhang, Q., Davis, S.J., Liu, F., Zheng, B., Geng, G., Xue, T.a., Li, M., Hong, C., Lu, Z., Streets, D.G., Guan, D., He, K., 2018. Targeted emission reductions from global super-polluting power plant units. Nat. Sustain. 1 (1), 59–68.

Wang, T., Huang, X., Wang, Z., Liu, Y., Ding, A., 2020. Secondary aerosol formation and its linkage with synoptic conditions during winter haze pollution over eastern China. Sci. Total Environ. 730, 138888.

Xia, Y., Zhao, Y., Nielsen, C.P., 2016. Benefits of China's efforts in gaseous pollutant control indicated by the bottom-up emissions and satellite observations 2000-2014. Atmos. Environ. 136, 43–53.

Yang, Y., Zhao, Y., Zhang, L., Lu, Y., 2019. Evaluating the methods and influencing factors of satellite-derived estimates of NOx emissions at regional scale: A case study for Yangtze River Delta, China. Atmos. Environ. 219, 117051.

Zhang, Y., Bo, X., Zhao, Y., Nielsen, C.P., 2019. Benefits of current and future policies on emissions of China's coal-fired power sector indicated by continuous emission monitoring. Environ. Pollut. 251, 415–424.

Zhang, L., Zhao, T., Gong, S., Kong, S., Tang, L., Liu, D., Wang, Y., Jin, L., Shan, Y., Tan, C., 2018. Updated emission inventories of power plants in simulating air quality during haze periods over East China. Atmos. Chem. Phys. 18 (3), 2065–2079.

Zhao, Y., Wang, S., Duan, L., Lei, Y., Cao, P., Hao, J., 2008. Primary air pollutant emissions of coal-fired power plants in China: Current status and future prediction. Atmos. Environ. 42 (36), 8442–8452.

Zhao, Y., Wang, S., Nielsen, C.P., Li, X., Hao, J., 2010. Establishment of a database of emission factors for atmospheric pollutants from Chinese coal-fired power plants. Atmos. Environ. 44 (12), 1515–1523.

Zheng, B., Cheng, J., Geng, G., Wang, X., He, K., 2021. Mapping anthropogenic emissions in China at 1 km spatial resolution and its application in air quality modeling. Science Bulletin 66 (6), 612–620.

Zhou, Y., Zhao, Y., 2015. Establishment of a high-resolution emission inventory and its impact assessment on air quality modeling in Jiangsu Province. AGU Fall Meeting Abstracts, China, pp. A51B–0027.